19th AIAA Computational Fluid Dynamics
22 - 25 June 2009, San Antonio, Texas

AIAA 2009-4000

Data Mining of Pareto-Optimal Transonic Airfoil Shapes Using Proper Orthogonal Decomposition

Akira Oyama[1]
Institute of Space and Astronautical Science, Japan Aerospace Exploration Agency, Sagamihara 229-8510, Japan

Taku Nonomura[2]
University of Tokyo, Sagamihara 229-8510, Japan

and

Kozo Fujii[3]
Institute of Space and Astronautical Science, Japan Aerospace Exploration Agency, Sagamihara 229-8510, Japan

A new approach to extract useful design information from Pareto-optimal solutions of optimization problems is proposed and applied to an aerodynamic transonic airfoil shape optimization. The proposed approach enables an analysis of line, face, or volume data of all Pareto-optimal solutions such as shape and flow field by decomposing the data into principal modes and corresponding base vectors using proper orthogonal decomposition (POD). Analysis of the shape and surface pressure data of the Pareto-optimal solutions of an aerodynamic transonic airfoil shape optimization problem showed that the optimized airfoils can be categorized into two families (low drag designs and high lift designs), where the lift is increased by changing the camber near the trailing edge among the low drag designs while the lift is increased by moving the lower surface upward among the high lift designs.

Nomenclature

$a_m(n)$	=	eigenvector of mode *m*
c	=	chord length
C_d	=	drag coefficient
C_l	=	lift coefficient
C_p	=	surface pressure coefficient
j	=	index of the grid points
$jmax$	=	number of the grid points
m	=	index of the modes
$mmax$	=	number of the modes ($mmax$=$nmax$)
n	=	index of the Pareto-optimal solutions
$nmax$	=	number of the Pareto-optimal solutions
$q(j,n)$	=	data of the Pareto-optimal solution n at grid point j to be analyzed by POD
$q_{l/d\_ave}(j)$	=	data of the lift-to-drag-ratio maximum design at grid point j
$q'(j,n)$	=	fluctuation of the data q of the Pareto-optimal solution n at grid point j
$q'_{base}(j,m)$	=	orthogonal base vector of mode m
$S_{m1,m2}$	=	covariance of q'_{base} of mode $m1$ and mode $m2$
x	=	coordinate in the chordwise direction
y	=	coordinate in the normal direction

[1] Assistant Professor, Department of Space Transportation Engineering, 3-1-1 Yoshinodai, Member AIAA.
[2] Research Associate, Department of Aeronautics and Astronautics, 3-1-1 Yoshinodai, Member AIAA.
[3] Professor, Department of Space Transportation Engineering, 3-1-1 Yoshinodai, Fellow AIAA.

I. Introduction

MULTIOBJECTIVE design exploration[1] (MODE) is a framework to extract essential knowledge of a multiobjective design optimization problem such as tradeoff information between contradicting objectives and the effect of each design parameter on the objectives. In the framework of MODE, Pareto-optimal solutions are obtained by multiobjective optimization using, for example, a multiobjective evolutionary algorithm[2], and then important design knowledge is extracted by analyzing objective function and design parameter values of the obtained Pareto-optimal solutions using so-called data mining approaches such as the self-organizing map[3] (SOM) and analysis of variance[4]. Recently, MODE framework has been applied to a wide variety of design optimization problems including multidisciplinary design of a regional-jet wing[5,6], aerodynamic design of the fly-back booster of a reusable launch vehicle[7], aerodynamic design of a flapping airfoil[8], and aerodynamic design of a turbine blade for a rocket engine[9].

However, data mining of objective function and design parameter values is not sufficient. One reason is that the design knowledge of a shape design optimization problem one can obtain depends on how the shape is parameterized. For example, if an airfoil shape is represented by B-Spline curves and coordinates of the corresponding control points are considered as the design parameters, it is difficult to obtain design knowledge related to leading edge radius, thickness distribution, and so on. Another reason is that data mining of the objective function and design parameter values does not lead to understanding of physics behind the design problem. For example, if one analyzes only design parameters of a transonic airfoil, he/she may not be able to understand relation between generation of shock wave and aerodynamic characteristics. To date, there is no efficient approach for analyzing such information as far as the authors know. The current approach is limited to shape and flow visualization of a limited number of samples of the obtained Pareto-optimal solutions.

Thanks to recent improvements in flow measurement techniques and computer performance, the interest of many fluid dynamics researchers is shifting from steady to unsteady flow. Because unsteady flow data are huge four-dimensional time-space data, one of the important research topics in this field is how to extract the dominant features of the unsteady flow data. Recently, proper orthogonal decomposition (POD, known as the Karhunen-Loeve expansion in pattern recognition, and principal component analysis in the statistical literature) has been used to analyze the unsteady flow data such as the vorticity fields of a flow in a flume[10], jet/vortex interaction[11], and flow in chemical processing equipment[12]. POD is a statistical approach that can extract dominant features in data by decomposing the data into a set of optimal orthogonal base vectors of decreasing importance. These base vectors are optimal in the sense that any other set of orthogonal base vectors cannot capture more information than the orthogonal base vectors obtained by POD as long as the number of base vectors is limited.

In the last decade, POD has also been used for design optimization[13-18]. In Refs. 13 and 14, POD is used to reduce the computational cost required to solve the Euler equations. In Refs. 15 and 16, POD is used to recognize the most contradicting objective functions and to reduce the number of objective functions in various problems. Refs. 17 and 18 propose to use POD to reduce the number of design parameters. In these references, eigenvectors of principal modes obtained by applying POD to the user-defined design parameters are considered as new design parameters. The motivation of all the above listed research into the application of POD to design optimization is the improvement of optimization efficiency.

The objective of the present study is to propose a new approach to extract useful design information from line, face, or volume data of Pareto-optimal solutions of optimization problems, and to apply this approach to aerodynamic transonic airfoil shape optimization data to extract knowledge related to aerodynamic transonic airfoil design. The proposed approach enables analysis of the shape and flow data of all Pareto-optimal solutions by decomposing the data into principal modes and eigenvectors using POD.

II. Pareto-Optimal Solutions

The Pareto-optimal solutions of the following design optimization problem are analyzed.

Objective functions:	lift coefficient (maximization)
	drag coefficient (minimization)
Constraints:	lift coefficient must be greater than 0
	maximum thickness must be greater than 0.10 chord length
Design parameters:	coordinates of 6 control points of the B-Spline curves representing an airfoil shape (Fig. 1)
Flow conditions:	free stream Mach number of 0.8
	Angle of attack of 2 degrees

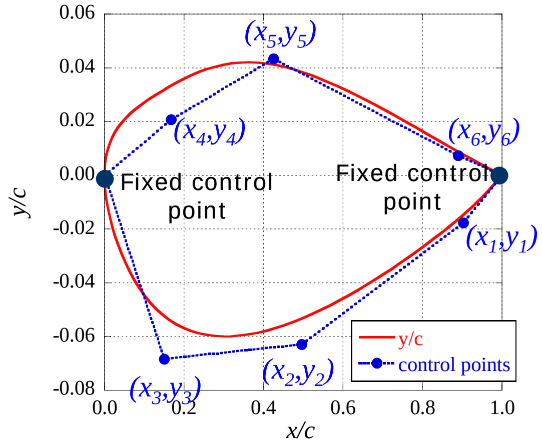

Figure 1. Parameterization of the airfoil shape. *Coordinates of 6 control points of the B-Spline curves representing an airfoil shape are considered as design parameters.*

Table 1. Search range of each design parameter

Design parameter	lower bound	upper bound
x_1	0.66	0.99
x_2	0.33	0.66
x_3	0.01	0.33
x_4	0.01	0.33
x_5	0.33	0.66
x_6	0.66	0.99
y_1	-0.1	0.10
y_2	-0.1	0.10
y_3	-0.1	0.10
y_4	0.0	0.20
y_5	0.0	0.20
y_6	0.0	0.20

The Pareto-optimal solutions are obtained by a multiobjective evolutionary algorithm (MOEA) used in Ref. 8. The present MOEA adopts real number coding because the optimization problem considered here is a real number optimization problem. The population size is kept at 64 and the maximum number of generations is set to 60. The initial population is generated randomly so that the initial population covers the entire design space presented in Table 1. The fitness of each design candidate is computed according to Pareto-ranking, fitness sharing, and Pareto-based constraint handling[19] based on its objective function and constraint function values. Here, Fonseca and Fleming's Pareto-based ranking method[20] and the fitness sharing method of Goldberg and Richardson[21] are used for Pareto-ranking where each individual is assigned a rank according to the number of individuals dominating it. In Pareto-based constraint handling, the rank of feasible designs is determined by the Pareto-ranking based on the objective function values, while the rank of infeasible designs is determined by the Pareto-ranking based on the constraint function values. Parents of the new generation are selected through roulette selection[22] from the best 64 individuals among the present generation and the best 64 individuals in the previous generation. A new generation is reproduced through crossover and mutation operators. The term "crossover" refers to an operator which combines the genotype of the selected parents and produces new individuals with the intent of improving the fitness value of the next generation. Here, the blended crossover[23], where the value of α is 0.5, is used for crossover between the selected solutions. Mutation is applied to the design parameters of the new generation to maintain diversity. Here, the probability of mutation taking place is 20%; this adds a random disturbance to the corresponding gene of up to 10% of the given range of each design parameter. The capability of the present MOEA to find quasi-optimal solutions has been well validated[24, 25].

The lift and drag coefficients of each design candidate are evaluated using a two-dimensional Reynolds-averaged Navier-Stokes solver. This code employs total variation diminishing type upwind differencing[26], the lower-upper symmetric Gauss-Seidel scheme[27], the turbulence model of Baldwin and Lomax[28] and the multigrid method[29].

All the design candidates and Pareto-optimal solutions are plotted in Fig. 2. The number of Pareto-optimal solutions obtained is 85. A strong tradeoff between lift maximization and drag minimization is observed. The static pressure distributions around the maximum lift, maximum lift-to-drag-ratio, and minimum drag airfoils are also shown in the figure. Figure 3 compares the shapes and surface pressure distributions of the above three designs. These figures indicate that the minimum drag design avoids generation of strong shock waves while the maximum lift design generates a strong and large negative pressure region. These figures also show that the maximum lift-to-drag-ratio design has a shape that is similar to supercritical airfoils. These facts indicate that the obtained Pareto-optimal solutions are good approximations of the true Pareto-optimal solutions.

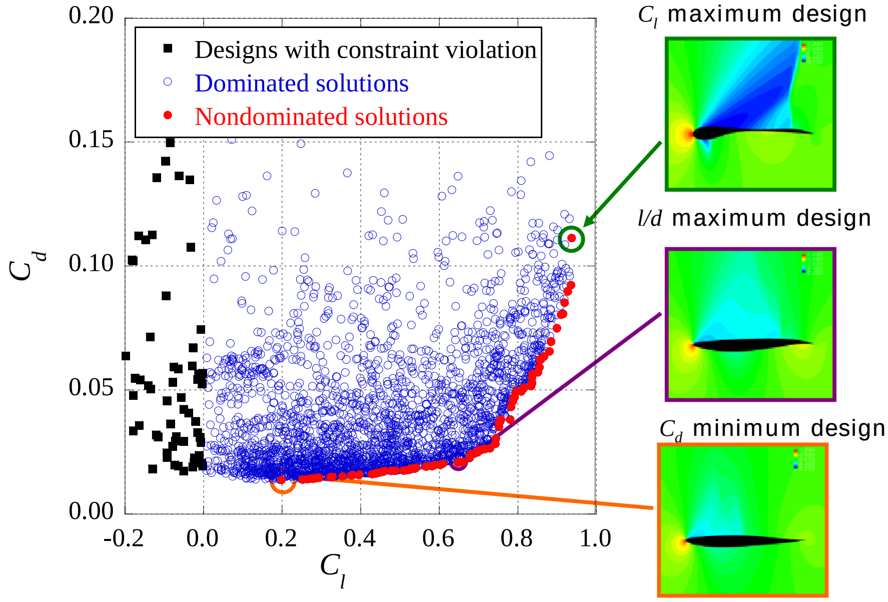

Figure 2. Distribution of the Pareto-optimal solutions and other design candidates with pressure distribution around the maximum lift, maximum lift-to-drag-ratio, and minimum drag airfoil.

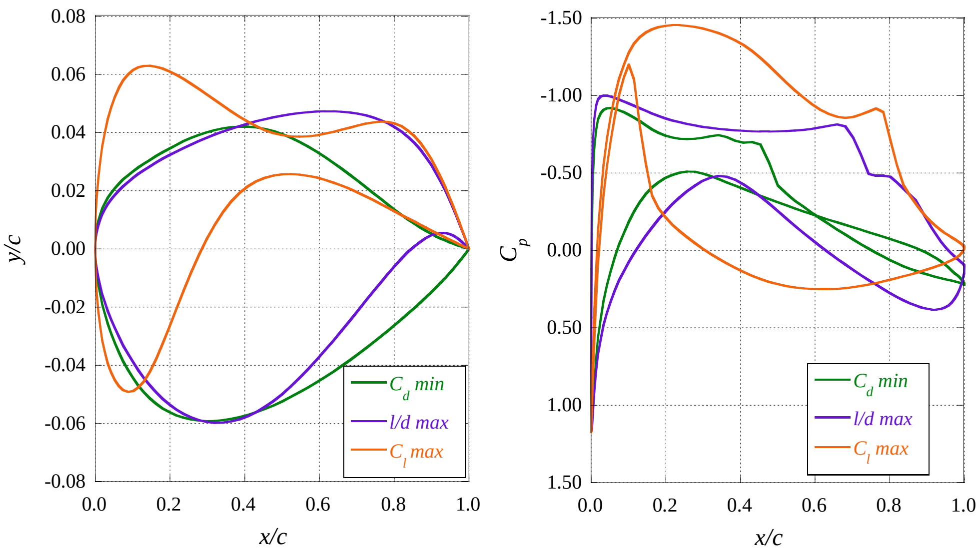

Figure 3. Shape and surface pressure distributions of the maximum lift, maximum lift-to-drag-ratio, and minimum drag airfoils.

III. Data Mining of Pareto-Optimal Solutions Using Proper Orthogonal Decomposition

In this study, shape and surface pressure data of the Pareto-optimal airfoils are analyzed using the snapshot POD proposed by Sirovich[30]. The Pareto-optimal solutions are numbered from the minimum drag design to the maximum lift design as shown in Fig. 4. The shape and surface pressure data analyzed here are *y* coordinates and the surface pressure on all grid points around the airfoil is as shown in Fig. 5. The number of grid points around an airfoil is 137.

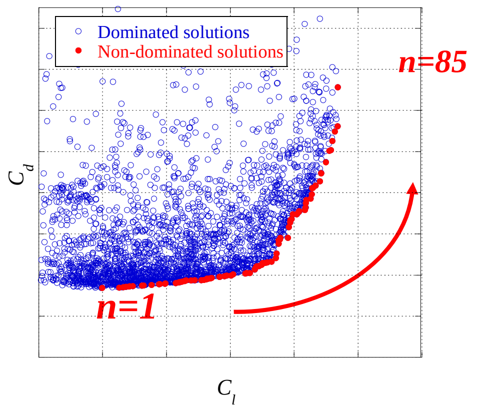

Figure 4. Index of the Pareto-optimal solutions. *For the minimum drag design, n=1; for the maximum lift design, n=nmax=85.*

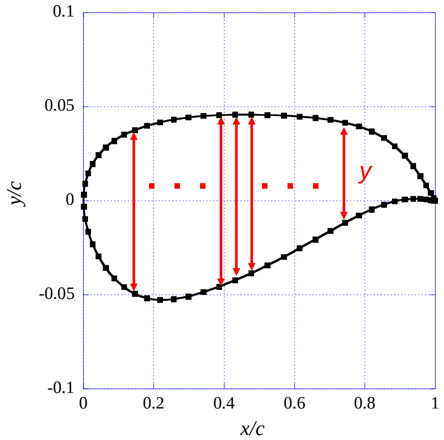

Figure 5. Definition of the shape data. *Shape data analyzed here are y coordinates defined on all grid points of the airfoil shape.*

In the original snapshot POD, the data to be analyzed are decomposed into the mean vector and the fluctuation vector from the mean vector to maximize variance. However, for analysis of Pareto-optimal solutions, it is not intuitive to understand the fluctuation from the mean shape or flow. Thus, it is reasonable to analyze the fluctuation from one representative design, for example, the median design. Here, the fluctuation from the lift-to-drag ratio maximum design is analyzed. The data of the Pareto-optimal solutions are decomposed into the data of the lift-to-drag-ratio maximum design and fluctuation data as

$$\begin{bmatrix} q(1,n) \\ q(2,n) \\ \vdots \\ q(j\max-1,n) \\ q(j\max,n) \end{bmatrix} = \begin{bmatrix} q_{l/d\_\max}(1) \\ q_{l/d\_\max}(2) \\ \vdots \\ q_{l/d\_\max}(j\max-1) \\ q_{l/d\_\max}(j\max) \end{bmatrix} + \begin{bmatrix} q'(1,n) \\ q'(2,n) \\ \vdots \\ q'(j\max-1,n) \\ q'(j\max,n) \end{bmatrix} \tag{1}$$

Then, the fluctuation vector is expressed by the linear sum of normalized eigenvectors and orthogonal base vectors:

$$\begin{bmatrix} q'(1,n) \\ q'(2,n) \\ \vdots \\ q'(j\max-1,n) \\ q'(j\max,n) \end{bmatrix} = a_1(n)\begin{bmatrix} q'_{base}(1,1) \\ q'_{base}(2,1) \\ \vdots \\ q'_{base}(j\max-1,1) \\ q'_{base}(j\max,1) \end{bmatrix} + \cdots + a_{m\max}(n)\begin{bmatrix} q'_{base}(1,m\max) \\ q'_{base}(2,m\max) \\ \vdots \\ q'_{base}(j\max-1,m\max) \\ q'_{base}(j\max,m\max) \end{bmatrix} \tag{2}$$

where each eigenvector is determined so that the energy defined by Eq. (3) is maximized.

$$\sum_{j=1}^{j\max} q'^2_{base}(j,m) \quad , m=1, 2, \ldots, mmax \tag{3}$$

The eigenvectors that maximize the energy defined by Eq. (3) can be obtained by solving the eigenvalue problem of the following covariance matrix:

$$\begin{pmatrix} S_{1,1} & \cdots & S_{m1,1} & \cdots & S_{m\max,1} \\ \vdots & \ddots & \vdots & & \vdots \\ S_{1,m2} & \cdots & S_{m1,m2} & \cdots & S_{m\max,m2} \\ \vdots & & \vdots & \ddots & \vdots \\ S_{1,m\max} & \cdots & S_{m1,m\max} & \cdots & S_{m\max,m\max} \end{pmatrix}$$

where

$$S_{m1,m2} = \sum_{j=1}^{j\max} q'(j,m1)q'(j,m2) \tag{5}$$

IV. Results

A. Data Mining of Airfoil Shapes Using POD

First, airfoil shape data of the Pareto-optimal solutions are analyzed. The shape data analyzed here are y coordinates defined on all grid points on the airfoil shape. The energy ratios of 10 principal orthogonal base vectors (principal POD modes) to the total energy are presented in Fig. 6. The first mode is dominant (more than 83%) and the first two modes represent more than 94% of the total energy.

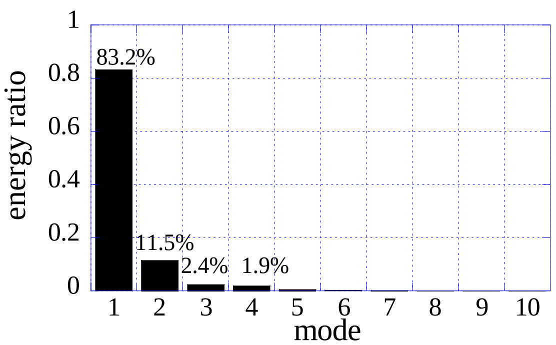

Figure 6. Energy ratio of the top 10 principal modes of the airfoil shape.

Figure 7 shows the components of the eigenvectors of the first four modes against the index of the non-dominated solutions n (left) and the lift coefficient $C_l(n)$ (right), respectively. This figure indicates that the obtained non-dominated airfoil shapes are categorized into two groups, i.e., the low drag designs (roughly $n<50$ and $C_l<0.75$) and the high lift designs ($n>50$ and $C_l>0.75$). As for the low drag designs, the second mode is dominant as the eigenvector of the first mode is almost zero. Among the high lift designs, the first mode is dominant as the eigenvector of the second mode is almost zero.

Figure 8 presents the lift-to-drag maximum airfoil shape and orthogonal base vectors of the first four modes. This figure indicates that the mode 1 mainly contributes to the most part of the lower surface change. The base vector of the mode 1 also indicates that thickness near the leading edge should be increased as the lower surface moves upward. This comes from the constraint on the maximum thickness imposed on the design optimization problem. The base vector of the second mode indicates that the second mode mainly contributes to the camber near the trailing edge. Recalling the shapes of the Pareto-optimal solutions are represented by equations (1) and (2), figures 7 and 8 indicate that the Pareto-optimal low drag designs increase lift by changing the camber near the trailing edge while the other part of the airfoil shape is almost fixed. As for the high lift designs, lift is increased by moving the lower surface upward without significant change in the trailing edge angle. This movement of the lower surface corresponds to camber increase. The thickness near the leading edge is increased as the lower surface moves upward to satisfy the constraint applied to the airfoil maximum thickness near the leading edge.

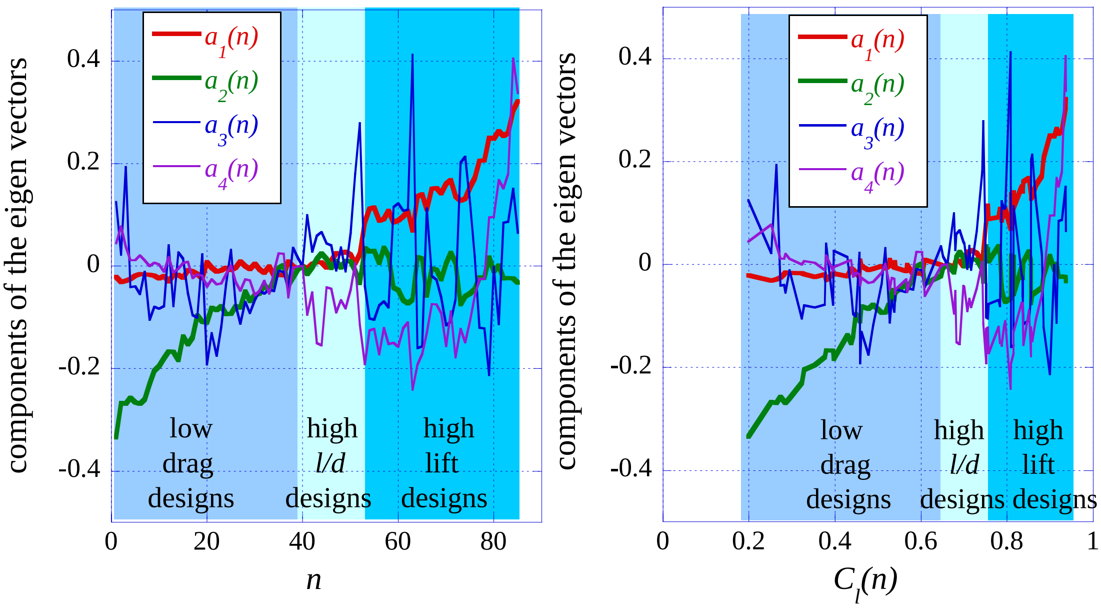

Figure 7. Eigenvectors of the first four modes of the airfoil shape against *n* (left) and $C_l(n)$(right).

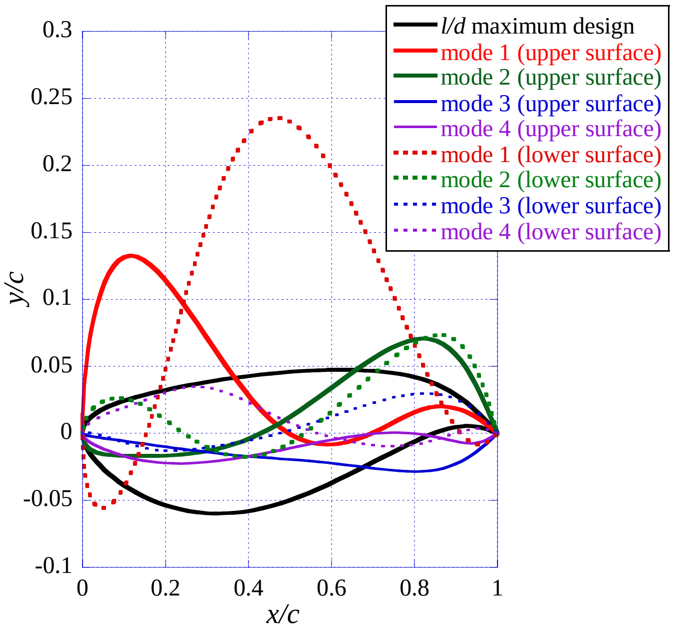

Figure 8. Shape of the lift-to-drag-ratio maximum airfoil design and the orthogonal base vectors of the first four modes of the airfoil shapes.

B. Data Mining of Surface Pressure Distribution Using POD

To demonstrate feasibility of the proposed approach for analyzing flow data, the simplest (one-dimensional) flow data, i.e., the surface pressure coefficient defined on all grid points on Pareto-optimal airfoil shapes is analyzed. The energy ratio of 10 principal orthogonal base vectors is presented in Fig. 9. The first mode is dominant (more than 78%) and the first two modes represent more than 93% of the total energy.

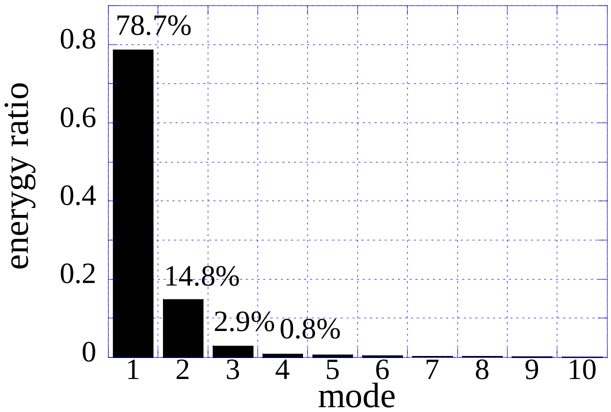

Figure 9. Energy ratio of the top 10 principal modes of the surface pressure coefficient distribution.

Components of the eigenvector of the first four modes are presented in Fig. 10. The eigenvectors of the first two modes are similar to those of the airfoil shape: the mode 2 is dominant for the low drag designs while the mode 1 is dominant for the high lift designs.

Figure 11 shows the surface pressure coefficient distribution of the lift-to-drag-ratio maximum design and the orthogonal base vectors of the first four modes. The second mode mainly contributes to the surface pressure of the trailing edge part of the airfoil. The eigen vectors and the base vectors presented in figs. 10 and 11 indicate that among the low drag designs, the lift increases due to the change in the surface pressure near the trailing edge. They also indicate that among the high lift designs, lift increases due to the surface pressure change from the leading edge to the trailing edge.

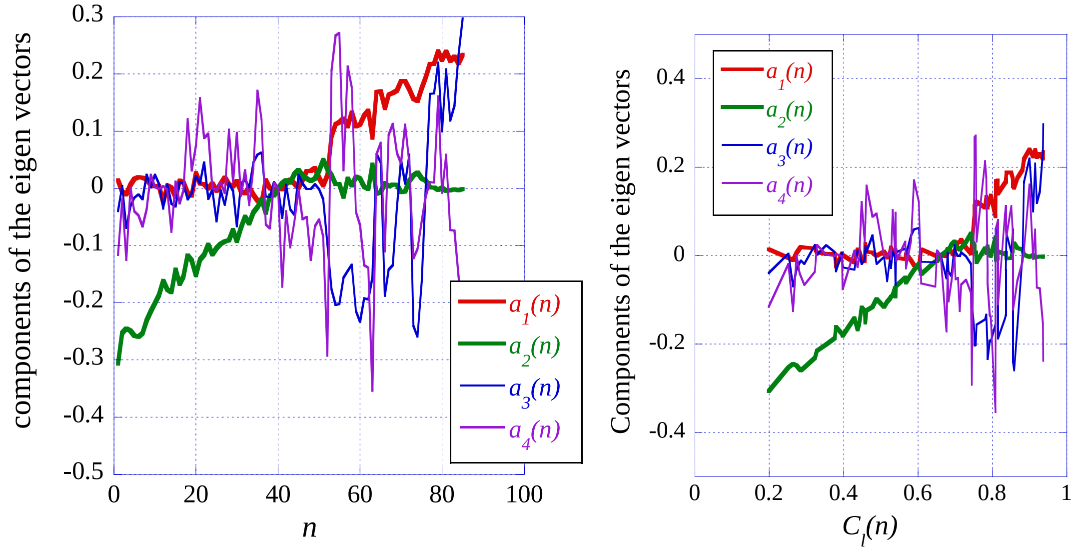

Figure 10. Eigenvectors of the first four modes of the surface pressure coefficient distribution.

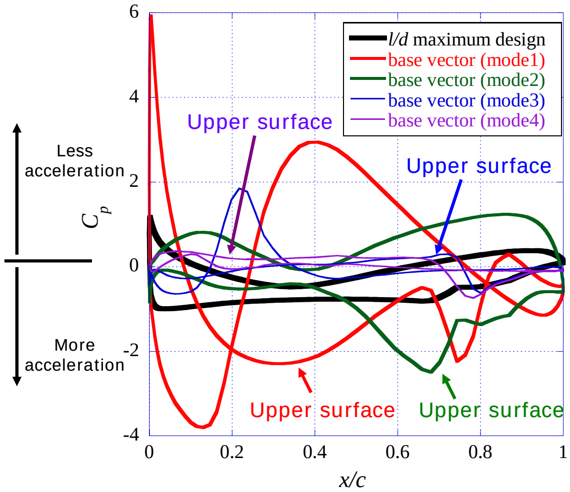

Figure 11. Surface pressure coefficient distribution of the lift-to-drag-ratio maximum airfoil design and the orthogonal base vectors of the first four modes of the surface pressure coefficient distribution.

V. Conclusions

A new approach to extract useful design information from line, face and volume data from the Pareto-optimal solutions of optimization problems has been proposed and applied to an aerodynamic transonic airfoil shape optimization. The proposed approach enables the analysis of line, face, and volume data of all Pareto-optimal solutions by decomposing the data of all Pareto-optimal solutions into principal modes and base vectors using POD.

Data mining of the shape and surface pressure data of the Pareto-optimal solutions of an aerodynamic transonic airfoil shape optimization problem showed that the optimized airfoils can be categorized into two families; low drag designs and high lift designs. Among the low drag designs, lift is increased by changing the camber near the trailing edge. Among the high lift designs, the lift is increased by moving the lower surface upward which corresponds to increase in the camber.

In this study, the feasibility of the proposed approach for shape and flow analysis of an aerodynamic transonic airfoil shape optimization problem is demonstrated. However, application of the present approach is not limited to aerodynamic designs. For example, in many thermal designs, structural designs, or image processing problems, objective function values are obtained from line, face, or volume data. Use of the proposed technique for analysis of such data will provide useful information.

Though the proposed method is applied to a two-objective optimization problem here, the proposed approach is also applicable to three or more objective optimization problems. The proposed approach should be more useful in the analysis of optimization problems involving three-dimensional flow or unsteady flow. In the near future the proposed approach will be applied to multidisciplinary turbine blade design and aerodynamic flapping wing design. As part of such research, analysis of all design candidates using the present method may also be of interest.

Acknowledgments

This research is partially supported by KAKENHI (20760552).

References

[1]Jeong, S., Chiba, K., and Obayashi, S., "Data Mining for Aerodynamic Design Space," *Journal of Aerospace Computing, Information, and Communication*, Vol. 2, No. 11, 2005, pp. 452-469.

[2] Deb, K., *Multiobjective Optimization Using Evolutionary Algorithms*, John Wiley & Sons, Ltd., Chichester, UK, 2001.

[3] Kohonen, T., *Self-Organizing Maps, 2nd ed.*, Springer, Heidelberg, Germany, 1997.

[4] Donald, R. J., Matthias, S., and William, J. W., "Efficient Global Optimization of Expensive Black-Box Function," *Journal Global Optimization*, Vol. 13, 1998, pp. 455-492.

[5]Chiba, K., Oyama, A., Obayashi, S., and Nakahashi, K., "Multidisciplinary Design Optimization and Data Mining for Transonic Regional-Jet Wing," *Journal of Aircraft*, Vol. 44, No. 4, 2007, pp. 110-1112.

[6]Chiba, K., and Obayashi, S., "Data Mining for Multidisciplinary Design Space of Regional-Jet Wing," *Journal of Aerospace Computing, Information, and Communication*, Vol. 4, No. 11, 2007, pp. 1019-1036.

[7]Obayashi, S., and Chiba, K., "Knowledge Discovery for Flyback-Booster Aerodynamic Wing Using Data Mining," *Journal of Spacecraft and Rockets*, Vol. 45, No. 5, 2008, pp. 975-987.

[8]Oyama, A., Okabe, Y., Fujii, K., Shimoyama, K., "A Study on Flapping Motion for MAV Design Using Design Exploration," AIAA-2007-2878, The AIAA Electronic Library [online database], URL: http://www.aiaa.org [cited 1 November 2008].

[9]Tani, N., Oyama, A., and Yamanishi, N., "Multiobjective Design Optimization of Rocket Engine Turbopump Turbine," Proceedings of the 5th International Spacecraft Propulsion Conference / 2nd International Symposium on Propulsion for Space Transportation [CD-ROM], 2008.

[10]Liberzon, A., Gurka, R., Tiselj, I., and Hetsroni, G., "Spatial Characterization of the Numerically Simulated Vorticity Fields of a Flow in a Flume," *Theoretical and Computational Fluid Dynamics*, Vol. 19, 2005, pp. 115-125.

[11]Maurel, S., Boree, J., and Lumley, J. L., "Extended Proper Orthogonal Decomposition: Application to Jet/Vortex Interaction," *Flow, Turbulence and Combustion*, Vol. 67, 2001, pp. 125-136.

[12]Tabib, M. V., and Joshi, J. B., "Analysis of Dominant Flow Structures and Their Flow Dynamics in Chemical Process Equipment Using Snapshot Proper Orthogonal Decomposition Technique," *Chemical Engineering Science*, Vol. 63, 2008, pp. 3695-3715.

[13]LeGresley, P. A., and Alonso, J. J., "Airfoil Design Optimization Using Reduced Order Models Based on Proper Orthogonal Decomposition," AIAA-2000-2545, The AIAA Electronic Library [online database], URL: http://www.aiaa.org [cited 1 November 2008].

[14]Goss, J., and Subbarao, K., "Inlet Shape Optimization Based on POD Model Reduction of the Euler Equations," AIAA 2008-5809, The AIAA Electronic Library [online database], URL: http://www.aiaa.org [cited 1 November 2008]..

[15]Deb, K., and Saxena, D. K., "Searching for Pareto-optimal solutions through dimensionality reduction for certain large-dimensional multiobjective optimization problems," IEEE Congress on Evolutionary Computation 2006, 2006.

[16]Jeong, S., Lim, J. N., Obayashi, S., and Koishi, M., "Design Exploration into a Tire Noise Reduction Problem," International Workshop on Multidisciplinary Design Exploration in Okinawa 2006, Okinawa, Japan, 2006.

[17]Toal, D. J. J., Bressloff, N. W., and Keane, A. J., "Geometric Filtration Using POD for Aerodynamic Design Optimization," AIAA-2008-6584, The AIAA Electronic Library [online database], URL: http://www.aiaa.org [cited 1 November 2008].

[18]Li, G., Li, M., Azarm, S. Rambo, J., and Joshi, Y., "Optimizing thermal design of data center cabinets with a new multiobjective genetic algorithm," *Distributed Parallel Databases*, Vol. 21, 2007, pp. 167-192.

[19]Oyama, A., Shimoyama, K., and Fujii, K., "New Constraint-Handling Method for Multi-objective Multi-Constraint Evolutionary Optimization," *Transactions of the Japan Society for Aeronautical and Space Sciences*, Vol. 50, No. 167, 2007, pp. 56-62.

[20]Fonseca, C. M., and Fleming, P. J., "Genetic Algorithms for Multiobjective Optimization: Formulation, Discussion and Generalization," *Proceedings of the 5th International Conference on Genetic Algorithms*, edited by Forrest, S., Morgan Kaufmann Publishers, Inc., San Mateo, CA, 1993, pp. 416-423.

[21]Goldberg., D. E., and Richardson, J., "Genetic Algorithms with Sharing for Multimodal Function Optimization", *Proceedings of the Second International Conference on Genetic Algorithms*, Lawrence Erlbaum Associates, Inc., Mahwah, New Jersey, 1987.

[22]Goldberg., D. E., *Genetic Algorithms in Search, Optimization and Machine Learning*, Addison-Wesley Publishing Company, Inc., Reading, MA, 1989.

[23]Eshelman, L. J., and Schaffer, J. D., "Real-Coded Genetic Algorithms and Interval Schemata," *Foundations of Genetic Algorithms 2*, edited by Whitley, L. D., Morgan Kaufmann Publishers, Inc., San Mateo, CA, 1993, pp. 187-202.

[24]Obayashi, S., Sasaki, D., and Oyama, A., "Finding Tradeoffs by Using Multiobjective Optimization Algorithms," *Transactions of the Japanese Society for Aeronautical and Space Sciences*, Vol. 27, 2004, pp. 51-58.

[25]Oyama, A., and Liou, M.S., "Multiobjective Optimization of Rocket Engine Pumps Using Evolutionary Algorithm," *AIAA Journal of Propulsion and Power*, Vol. 18, No. 3, 2002, pp. 528-535.

[26]Obayashi, S. and Wada, Y., "Practical Formulation of a Positively Conservative Scheme," *AIAA Journal*, Vol. 32, No. 5, 1994, pp.1093-1095.

[27]Obayashi, S. and Guruswamy, G. P., "Convergence Acceleration of an Aeroelastic Navier-Stokes Solver," *AIAA Journal*, Vol. 33, No. 6, 1995, pp.1134-1141.

[28]Baldwin, B. S. and Lomax, H., "Thin-Layer Approximation and Algebraic Model for Separated Turbulent Flows," AIAA-1978-0257, The AIAA Electronic Library [online database], URL: http://www.aiaa.org [cited 1 November 2008], 1985.

[29]Brant, A., "Multi-Level Adaptive Solutions to Boundary Value Problems," *Mathematics of Computation*, Vol. 31, No. 138, 1977, pp.333-390.

[30]Sirovich, L., "Turbulence and Dynamics of Coherent Structures Part 1: Coherent Structures," *Quarterly of Applied Mathematics*, Vol. 45, No. 3, 1987, pp. 561-571.